The Shapes and Other Properties of Non-Transition Element Complexes. 3. AB_5

Benjamin M. Gimarc

Contribution from the Department of Chemistry, University of South Carolina, Columbia, South Carolina 29208. *Received December 27, 1976*

Abstract: A qualitative molecular orbital model of the valence electronic structures of pentacoordinate halide complexes AB_5 of non-transition elements is developed based on the results of extended Hückel calculations for simple AB_5 systems. The model is used to explain the observed trigonal bipyramidal and square pyramidal shapes of AB_5 complexes. Variations in bond distances and bond angles are discussed. A simple scheme is used to predict the relative heights of barriers to Berry pseudorotation in trigonal bipyramidal AB_5 complexes. Barriers to inversion and intramolecular ligand exchange are compared for AB_3, AB_4, and AB_5 complexes. Relative stabilities of AB_4, AB_5, and AB_6 complexes are compared and rationalized using molecular orbital correlation diagrams.

In this paper a qualitative molecular orbital (MO) model of electronic structure will be used to explain, rationalize, and predict the structures and other properties of non-transition element complexes of the general formula AB_5. This study is limited to those complexes in which the central atom A is of the elements from the main groups 3 through 0 of the periodic table and the ligands B are single atoms, usually halogens. Tables I and II list the known halide complexes. The rules of qualitative MO theory have been discussed elsewhere.[1,2]

In the model presented here the AO basis set consists of the s and p valence AOs of the central atom A and one AO from each ligand B appropriate for the formation of a σ bond to the central atom. For AB_5 complexes this is a total of nine AOs from which nine MOs can be formed. The valence electrons are counted by including all of those in the valence s and p AOs of the neutral central atom plus one electron from each halogen ligand (none from oxygen ligands) plus one electron for each negative charge on the complex (subtract positive charges). Comparable studies have been done for the series AB_6[2] and AB_4.[3]

Table I lists the complexes with ten valence electrons. These complexes are mainly trigonal bipyramidal (D_{3h}) in structure with the bonds to the axial ligands ($A-B_{ax}$) being slightly longer than those to the equatorial ligands ($A-B_{eq}$).[4-9] Table III contains the bond distances that are known for the trigonal bipyramidal ten-electron complexes. Not all ten-electron AB_5

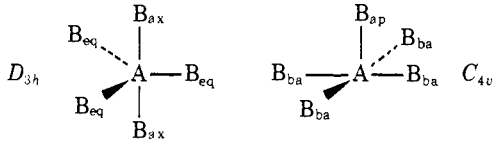

complexes have the D_{3h} structure in one or more phases. For example, although $SbCl_5$ is monomeric and trigonal bipyramidal in the gaseous, liquid, and solid states,[8,10,11] PCl_5 is D_{3h} in the gas[6] and in liquid solutions[12] but in the solid it has the ionic form $PCl_4^+PCl_6^-$.[13] Solid PBr_5 is $PBr_4^+Br^-$.[14] In the crystalline state BiF_5[15,16] and GeF_5^-[17] consist of infinite chains of AB_5 units in which the central atom A is approximately octahedrally coordinated. More serious exceptions to trigonal bipyramidal geometry arise with $InCl_5^{2-}$ and $TlCl_5^{2-}$.[18-23] In the crystal, isolated $InCl_5^{2-}$ ions occur with square pyramidal geometry (C_{4v}). The bond to the apical chlorine ($A-B_{ap}$) is 2.415 Å and the somewhat longer basal chlorine bonds ($A-B_{ba}$) are 2.456 Å. The angle between apical and basal chlorines is 107.87°. The In atom is said to be above the basal plane of the square pyramid. $TlCl_5^{2-}$ is also square pyramidal.

The energy of the square pyramidal (C_{4v}) structure must not be far above that of the trigonal bipyramidal (D_{3h}) shape for the more characteristic members of the ten-electron series. NMR studies of PF_5, PCl_5,[24] $SbCl_5$, and SiF_5^-[25] indicate that all ligands are structurally equivalent on the NMR time scale despite the fact that axial and equatorial ligands are known from other structural studies to occupy positions with different electronic environments. Berry proposed a pseudorotation mechanism of intramolecular ligand exchange to account for the observed NMR equivalence.[24] In the picture shown here,

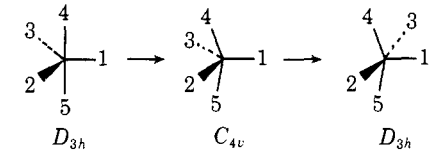

the axial ligands 4 and 5 on the left become equatorial on the right while equatorial ligands 2 and 3 become axial. The energy barriers to pseudorotation have been estimated to be on the order of a few kcal/mol. Other mechanisms for intramolecular ligand exchange have been suggested including a process called the turnstile mechanism.[26] Here the trigonal bipyramid is assumed to distort to a structure of C_s symmetry, then ligands 2, 3, and 4 rotate by 60° about a pseudothreefold axis, like a turnstile, to another C_s structure that can relax to the bipyramidal shape with resulting exchange of axial and equatorial ligands.

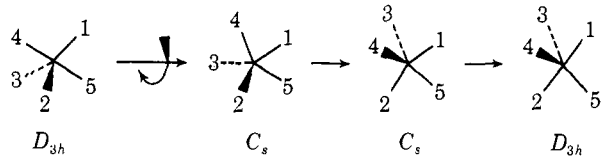

A number of mixed ligand complexes are known in the ten-electron bipyramidal AB_5 series. These include PF_nCl_{5-n},[27] ClO_2F_3,[28] IO_2F_3,[29] and SOF_4.[30] The most stable configuration in each case has the more electronegative ligands in the axial positions.[4]

The 12-electron AB_5 complexes listed in Table II are square pyramidal (C_{4v}). The bond to the apical ligand in each of these complexes is 0.1-0.2 Å shorter than the bonds to the basal ligands. The angle between apical and basal ligands is less than 90°, usually around 80°, and the central atom is said to be below the basal plane of the square pyramid, unlike that of the ten-electron square pyramidal structure of $InCl_5^{2-}$. Table IV collects the experimental bond distances and angles.[31-35] Apical-basal intramolecular ligand exchange has not been observed in the 12-electron AB_5 complexes.

Examples of mixed ligand complexes of the 12-electron series are $ClOF_4^-$,[36] IOF_4^-,[37] $XeOF_4$,[38] and $TeOF_4^{2-}$.[39] In these complexes the apical position is occupied by the less electronegative ligand.

0002-7863/78/1500-2346$01.00/0

Table I. Known AB_5 Complexes. Ten Valence Electrons

3	4	5	6	7	0
AlF_5^{2-}	SiF_5^-	PF_5			
	$SiCl_5^-$	PCl_5			
		PBr_5			
GaF_5^{2-}	GeF_5^-	AsF_5			
	$GeCl_5^-$				
InF_5^{2-}		SbF_5			
$InCl_5^{2-}$	$SnCl_5^-$	$SbCl_5$			
	$SnBr_5^-$				
		BiF_5			
$TlCl_5^{2-}$					

Table II. Known AB_5 Complexes. 12 Valence Electrons

3	4	5	6	7	0
			SF_5^-	ClF_5	
			SeF_5^-	BrF_5	
			$SeCl_5^-$		
			$SeBr_5^-$		
		SbF_5^{2-}	TeF_5^-	IF_5	XeF_5^+
		$SbCl_5^{2-}$	$TeCl_5^-$		
		$SbBr_5^{2-}$	$TeBr_5^-$		
		SbI_5^{2-}			
		$BiCl_5^{2-}$			
	$PbBr_5^{3-}$	$BiBr_5^{2-}$			
		BiI_5^{2-}	PoI_5^-		

Table III. Bond Distances (Å) for 10-Electron AB_5 Complexes in the Trigonal Bipyramidal Structure

	$SnCl_5^-$ [a]	PF_5 [b]	PCl_5 [c]	AsF_5 [d]	$SbCl_5$ [e]
$A-B_{ax}$	2.38	1.577	2.124	1.711	2.34
$A-B_{eq}$	2.36	1.534	2.020	1.656	2.29

[a] Reference 9. [b] Reference 5. [c] Reference 6. [d] Reference 7. [e] Reference 8.

Table IV. Bond Distances (Å) and Angles (deg) for 12-Electron AB_5 Complexes in Square Pyramidal Geometry

	SbF_5^{2-} [a]	TeF_5^- [b]	IF_5 [c]	XeF_5^+ [d]	BrF_5 [c]	$SbCl_5^{2-}$ [e]
$A-B_{ap}$	1.916	1.862	1.844	1.793	1.689	2.356
$A-B_{ba}$	2.075	1.953	1.869	1.845	1.774	2.636
$B_{ap}-A-B_{ba}$	79.4	78.9	81.9	79.0	84.8	85.2

[a] Reference 31. [b] Reference 32. [c] Reference 33. [d] Reference 34. [e] Reference 35.

The 11-electron radicals SF_5,[40] PF_5^-,[41] and PCl_5^- [42] are known. These are believed to have square pyramidal C_{4v} structures.

There have been many theoretical studies of the properties of AB_5 species. Hoffmann, Howell, and Meutterties[43] have already given a qualitative discussion of the properties of the phosphoranes based on the results of extended Hückel calculations for PH_5. Their paper is very close in inspiration and in a number of details to the work to be described here but their concern was limited to the ten-electron AB_5 series (phosphoranes). Rossi and Hoffmann[44] have recently published a similar study of transition metals pentacoordinated with ligands such as CO, NO, and O_2, an area completely avoided here. Bartell[45a] and Pearson[45b] have used a symmetry rule based on the second-order or pseudo-Jahn-Teller effect to compare trigonal bipyramidal and square pyramidal shapes for AB_5 complexes. Musher[46] and Shustorovich and Buslaev[47] have also presented qualitative studies of AB_5 complexes including some limited comparisons with AB_4 and AB_6 systems.

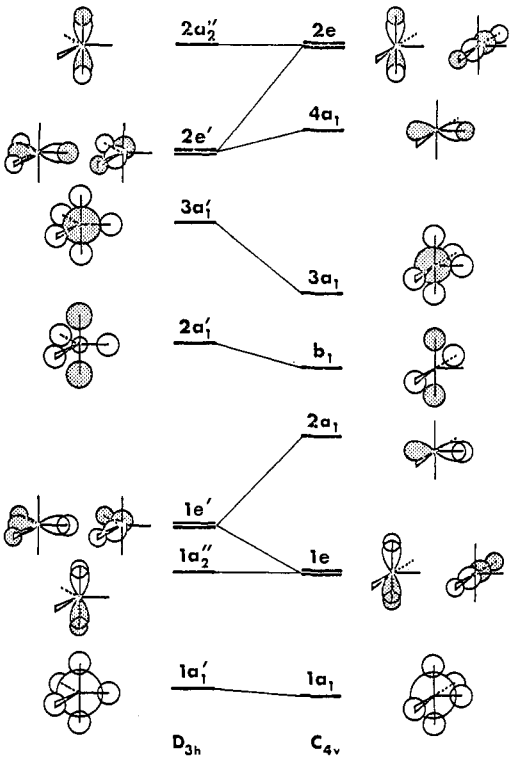

Figure 1. MO correlations for AB_5 complexes in trigonal bipyramidal (D_{3h}) and square pyramidal (C_{4v}) shapes.

The conclusions of a large number of AB_5 calculations are remarkably consistent.[48-64] The 12-electron ClF_5 complex is strongly square pyramidal (C_{4v}), not trigonal bipyramidal (D_{3h}). The ten-electron AB_5 systems prefer D_{3h} to C_{4v} geometry but only by a few kcal/mol. Calculated bond orders to axial positions in the D_{3h} structure are smaller than those to equatorial positions and, where geometries were obtained by total energy minimizations, the axial bonds are longer than the equatorial bonds. The calculated charge densities at the axial positions are more negative than those at the equatorial positions, indicating preferred axial sites for substitution of electronegative ligands. When Berry pseudorotation and turnstile mechanisms of intramolecular ligand exchange are compared for the phosphoranes or their analogues the C_{4v} transition state of the pseudorotation mechanism turns out to be several kcal/mol lower than C_s structures for the turnstile mechanism. Finally, all of these conclusions appear to be qualitatively insensitive to whether or not central atom d AOs were included in the basis set.

Molecular Orbitals and Molecular Shapes

AO composition diagrams of the MOs of D_{3h} geometry are shown in Figure 1. The energy order of the MOs in Figure 1 as well as those in other figures in this paper are given by extended Hückel calculations on model AH_5 systems. The lowest energy MO is the bonding orbital $1a_1'$ composed of the central atom s and the ligand AOs all overlapping in phase. The corresponding antibonding MO is $3a_1'$, with all five ligand AOs of opposite phase to that of the central atom s AO making the $3a_1'$ orbital high in energy. In $1a_2''$ the central atom p AO that points along the threefold axis overlaps in phase the axial ligand AOs. The corresponding antibonding $2a_2''$ MO has the highest energy in the whole set. A system with a threefold symmetry axis must have doubly degenerate MOs. The lower energy degenerate set $1e'$ is composed of the central atom p AOs that lie in the equatorial plane overlapping in phase with the equatorial ligand AOs. The energy of $1e'$ is higher than that of $1a_2''$ because the overlap between the ligand AOs and the

central atom p orbital is poorer in 1e′ than it is in $1a_2''$. The antibonding 2e′ degenerate pair lies high in energy but below $2a_2''$.

Thus far we have formed eight of the nine MOs of the AB_5 (D_{3h}) set. The last MO turns out to have a_1' symmetry. One way to derive this orbital is by considering the symmetry-adapted basis functions of a_1' symmetry. Symmetry-adapted basis functions have the desired symmetry, in this case a_1', and they are composed of AO combinations in which only those AOs appear that have coefficients of equal magnitude as required by the symmetry of the group. Once in hand, the symmetry-adapted basis functions can be linearly combined or mixed to form MOs. There are only three symmetry-adapted functions of a_1' symmetry: h_1, h_2, and h_3. From the three a_1'

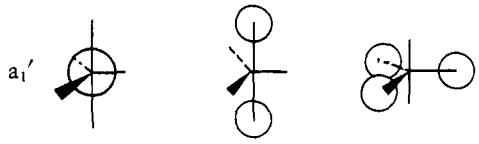

symmetry-adapted basis functions, linear combinations can produce only three linearly independent a_1' MOs. In both $1a_1'$ and $3a_1'$ we have combined h_2 and h_3 in phase with each other, then we mixed that combination either in phase with h_1 to form $1a_1' = h_1 + h_2 + h_3$, or out of phase with h_1 to make $3a_1' = h_2 + h_3 - h_1$. (In the MO combinations the symmetry-adapted basis functions do not appear with the same weight, but since we are primarily interested in phase relations we ignore the mixing coefficients that should appear before h_1, h_2, and h_3.) We already have two MOs with combination $h_2 + h_3$ so the third a_1' MO must have h_2 and h_3 of opposite phase: $h_3 - h_2$. But to the out-of-phase combination $h_3 - h_2$ we can match h_1 either in phase with h_3 or in phase with h_2. Thus, we get two possibilities: $a = h_3 - h_2 + h_1$ and $b = h_3 - h_2 - h_1$. Either of these combinations looks like the kind of MO that might lie in energy between $1a_1'$ and $3a_1'$. How do we choose between them? When Hoffmann, Howell, and Muetterties[43] faced this problem, they added a and b together to make c, canceling out

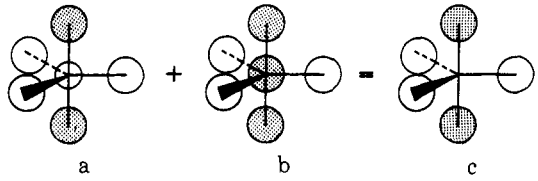

the central atom s AO. Indeed, Rauk, Allen, and Mislow[48] used a picture like c to represent the corresponding valence MO that they obtained from ab initio calculations for PH_5. The choice of c is appealing and, in fact, calculations yield a small central atom s AO coefficient, but that selection would discard some very useful information about $2a_1'$ that makes it different from the related b_1 MO of C_{4v} geometry. D_{3h} symmetry allows the central atom s AO to enter a_1' MOs and even though its contribution to $2a_1'$ may be small it will directly influence the energy of that MO. On the other hand, the central atom s coefficient of the related b_1 MO of C_{4v} symmetry must be zero. Figure 1 contains the picture $2a_1'$ (a) because of its lower energy and its explicit central atom s AO content.[70]

The C_{4v} structure is obtained from the D_{3h} shape by opening the angle between a pair of equatorial ligands from 120 to 180°. This makes the apical-basal angle 90°, simplifies energy comparisons, and serves as a compromise C_{4v} structure. The MOs of C_{4v} symmetry develop from those of D_{3h} geometry. Angular changes that increase AO overlap lower the MO energy. The energy of 1e (C_{4v}) is lower than that of 1e′ (D_{3h}) because overlap between the central atom p and ligand AOs is better in 1e (C_{4v}). The MO energy increases from 1e′ (D_{3h}) to $2a_1$ (C_{4v}) because a pair of ligand AOs in good overlap with the central atom p AO in one of the components of 1e′ (D_{3h}) move away from the p orbital lobe toward the MO nodal surface in $2a_1$ (C_{4v}). This is a large change in overlap, and therefore energy, compared to that of 1e′ (D_{3h})-1e (C_{4v}).

The $2a_1'$ (D_{3h})-b_1 (C_{4v}) orbital system requires special discussion. The central atom s and one of the equatorial ligand AOs drop out of $2a_1'$ (D_{3h}) when it becomes b_1 (C_{4v}) and the nodal surfaces move to cut through the base edges of the pyramid and intersect each other along the C_4 axis. The alternant phases of the basal ligand AOs of b_1 (C_{4v}) are the same as those of the axial and equatorial ligand AOs in the $2a_1'$ (D_{3h}) MO to which b_1 is related. Canceling A–B bonding and antibonding interactions should give $2a_1'$ (a) an energy in the nonbonding range and therefore comparable to b_1 (C_{4v}), but whether $2a_1'$ (D_{3h}) is above or below b_1 is uncertain from qualitative arguments alone.[70] One might be more confident in saying that $2a_1'$ (b) is higher than b_1. Extended Hückel[43] and ab initio[48] MO calculations on AB_5 model systems put $2a_1'$ (D_{3h}) slightly higher than b_1 (C_{4v}). The point here is that the energy difference between $2a_1'$ and b_1 is not usually large enough to control the molecular shape of ten-electron AB_5 complexes for which $2a_1'$-b_1 is the highest occupied MO. Instead, geometry is primarily determined by the steeply rising 1e′ (D_{3h})-$2a_1$ (C_{4v}) MO system just below.

The orbital correlation $3a_1'$ (D_{3h})-$3a_1$ (C_{4v}) also merits extra consideration. Opening the equatorial angle in $3a_1'$ (D_{3h}) moves equatorial ligands closer together and increases the overlaps in two pairs of ligand AOs. Although the overlaps themselves are not large, the ligand AO coefficients in $3a_1'$-$3a_1$ are large because of the complicated nature of the nodal surfaces in the orbitals and the large coefficients amplify the overlap change to make $3a_1$ (C_{4v}) considerably lower in energy than $3a_1'$ (D_{3h}). However, orbital mixing also acts to stabilize $3a_1$ (C_{4v}) relative to $3a_1'$ (D_{3h}). Symmetry eliminates any contribution to $3a_1'$ (D_{3h}) from the horizontal (equatorial) p AO of the central atom but this AO could add to $3a_1$ (C_{4v}). Similarly, no central atom s orbital can be included in 2e′ (D_{3h}), although it is allowed in $4a_1$ (C_{4v}). The orbitals $3a_1$ and $4a_1$ (C_{4v}) are the two highest energy MOs of a_1 classification and their AO compositions are different. Therefore, they should be mixed as shown in Figure 2. The after-mixing picture of $3a_1$ is formed by the superposition or summation $3a_1 + 4a_1$ of before-mixing pictures. Similarly, the after-mixing representation of $4a_1$ is the difference $3a_1 - 4a_1$ of before-mixing pictures. Mixing makes $3a_1$ an orbital with a large central atom lobe pointing out of the base of the square pyramid and of phase opposite to that of the four basal ligand AOs. The axial ligand AO contribution is reduced but not necessarily to zero as assumed in Figure 2. The perturbation effect of mixing is to lower the energy of $3a_1$ and raise that of $4a_1$. The after-mixing picture of $3a_1$ (C_{4v}) reminds one of the lone pair orbital of the valence shell electron pair repulsion (VSEPR) model.[65] Mixing also accounts for the higher than expected energy of $4a_1$ (C_{4v}) as shown in Figure 1. On overlap arguments alone one would have expected $4a_1$ (C_{4v}) to be lower than 2e′ (D_{3h}).

Consider the correlation diagram of Figure 1 as a whole. For ten-electron AB_5 complexes the highest occupied MO system is $2a_1'$ (D_{3h})-b_1 (C_{4v}). Although the energy slope of this system may favor the square pyramidal structure, the energy difference is not enough to overcome the steeply rising 1e′ (D_{3h})-$2a_1$ (C_{4v}) orbital of lower energy. It is the 1e′-$2a_1$ system that gives the ten-electron AB_5 complexes their trigonal bipyramidal geometry. The 12-electron complexes are square pyramidal because the $3a_1'$ (D_{3h})-$3a_1$ (C_{4v}) MO system is occupied.

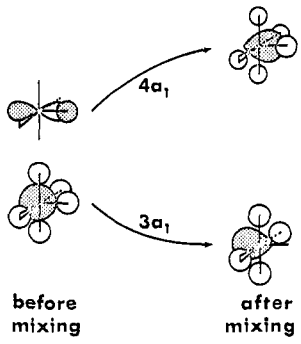

Figure 2. Orbital mixing provides more realistic representations of higher energy a_1 MOs for square pyramidal geometry.

The Barrier to Pseudorotation

Ligand exchange has been observed experimentally in a number of ten-electron AB_5 complexes. If this occurs by the Berry pseudorotation mechanism, and the best evidence indicates that it does, it is because the C_{4v} transition state is only a few kcal/mol above the D_{3h} structure for these complexes. The source of the pseudorotation barrier is the $1e'$ (D_{3h})-$2a_1$ (C_{4v}) MO in Figure 1, but this may be reduced or damped by the $2a_1'$ (D_{3h})-b_1 (C_{4v}) system above it. Now b_1 (C_{4v}) is the only MO of either symmetry that is composed of ligand AOs only and therefore independent of the energy of the central atom orbitals. The choice of a central atom of low electronegativity and therefore high energy s AO will raise the energy of $2a_1'$ (D_{3h}) but not b_1 (C_{4v}). The choice of more electronegative ligands with lower energy AOs will lower b_1 (C_{4v}) more than it will $2a_1'$ (D_{3h}). Thus by appropriate choices of ligands and central atoms we can control the barrier to pseudorotation. The rules are these: (1) Lower central atom electronegativity lowers the barrier. (2) Greater ligand electronegativity lowers the barrier. Consider the series PF_5, PCl_5, PBr_5. The ligand electronegativity rises relative to a constant central atom through this series. Since large ligand electronegativity favors a low pseudorotation barrier we predict that the barrier should increase as $PF_5 < PCl_5 < PBr_5$. Through the series PF_5, AsF_5, SbF_5 the electronegativity of the central atom decreases relative to the constant ligand. Since lower central atom electronegativity lowers the barrier, the order of barriers should be $SbF_5 < AsF_5 < PF_5$. Through the series SbF_5, $AsCl_5$, PBr_5 the central atom electronegativities increase and the ligand electronegativities decrease, both raising the barrier. Therefore, we predict the barriers should increase as $SbF_5 < AsCl_5 < PBr_5$. For the series PF_5, $AsCl_5$, $SbBr_5$, central atom electronegativities decrease favoring lower barriers while ligand electronegativities also decrease but favoring higher barriers. Because the effects oppose each other, no qualitative predictions are possible in this case.

How do these predictions compare with estimated barriers from experiment? In his original interpretation of NMR data for PF_5 and PCl_5, Berry[24] concluded that ligands exchange faster in PF_5 than in PCl_5 and therefore PF_5 must have a lower barrier than does PCl_5 or $PF_5 < PCl_5$, the order predicted by the qualitative model. Bernstein, Abramowitz, and Levin[66] have recently published a careful study of the vibrational spectra of PF_5 and AsF_5 and have calculated the potential functions for axial-equatorial exchange. They find $AsF_5 < PF_5$, which agrees with an earlier experimental study by Hoskins and Lord,[67] and checks the order predicted by the qualitative model. Holmes and co-workers[68] have published several tables of estimated barriers based on vibrational spectral data and various assumptions. Unfortunately, there are a number of reversals of relative barrier size in Holmes' results but two consistencies remain: $SbCl_5 < PCl_5$ and $SbCl_5 < AsF_5$. The first pair matches the order that would be predicted by the qualitative model while the second pair presents a comparison the qualitative model cannot make because of opposing effects. In their ab initio SCF MO studies of PH_5, Rauk, Allen, and Mislow[48] performed an additional calculation in which the nuclear charge on the hydrogens was increased from 1.0 to 1.1, making them slightly more electronegative. The effect was to lower slightly the barrier to pseudorotation compared to that for normal hydrogens. Once more, this is just what the qualitative model predicts would result from increasing the ligand electronegativity. Thus where more rigorous data are available for comparison, the qualitative MO predictions are correct.

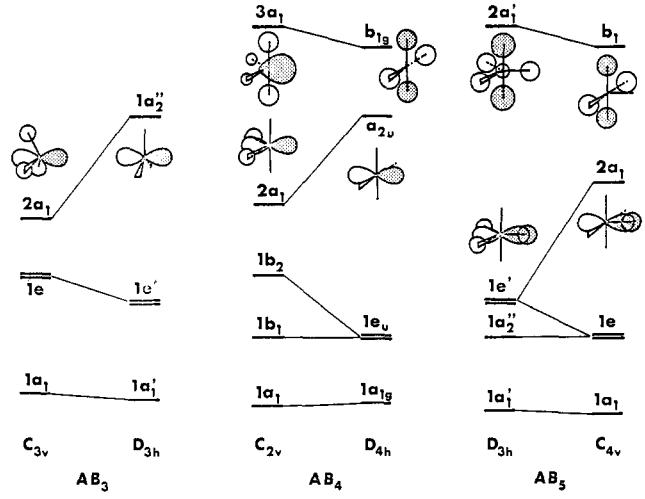

Figure 3. Comparison of higher occupied MOs and barriers to inversion and pseudorotation for AB_3 (8e), AB_4 (10e), and AB_5 (10e) complexes.

One should note that the pseudorotation phenomenon is one of ten-electron AB_5 complexes in general and not restricted to group 5 halides. For example, the qualitative model predicts the following increasing order of barriers: $AlF_5^{2-} < SiF_5^- < PF_5$. No experimental data are available for comparison.

Is it possible to make the energy of $2a_1'$ (D_{3h}) so high and that of b_1 (C_{4v}) so low that the pseudorotation barrier disappears entirely and the ten-electron complex is more stable in square pyramidal form? Among the elements considered here Tl has the highest energy valence s AO and combining ligands of lowest energy would yield TlF_5^{2-}. Unfortunately, this complex is not known but the closely related species $InCl_5^{2-}$ and $TlCl_5^{2-}$ both have square pyramidal shape. Other promising candidates for C_{4v} structures are PbF_5^- and $PbCl_5^-$, but these complexes are unknown.

NMR data indicate that the ten-electron complex SF_4 undergoes axial-equatorial ligand exchange through a Berry pseudorotation mechanism.[69] Barriers must be on the order of a few kcal/mol, comparable in size to those of the ten-electron AB_5 series. Although ten-electron AB_4 and AB_5 systems are floppy, the eight-electron AB_3 systems are much more rigid. Figure 3 shows the higher occupied MOs of AB_3, AB_4, and AB_5 in order to compare similarities and differences. The comparison is one between complexes formed from the same central atoms and ligands such as PF_3, PF_4^-, and PF_5. Rauk, Allen, and Mislow[48] present an ab initio based diagram for PH_3 and PH_5.

The origin of the inversion barrier is a strikingly similar MO in all three cases. It is the $2a_1$ (C_{3v})-$1a_2''$ (D_{3h}) MO system in AB_3, $2a_1$ (C_{2v})-a_{2u} (D_{4h}) in AB_4, and $1e'$ (D_{3h})-$2a_1$ (C_{4v}) in AB_5. In each instance the barrier results from ligand AOs moving away from the central atom p AO that lies along the principal symmetry axis of the transition state. At the top of the barrier, two or more ligands are on or near the nodal surface of the MO. But in the AB_4 and AB_5 cases a higher occu-

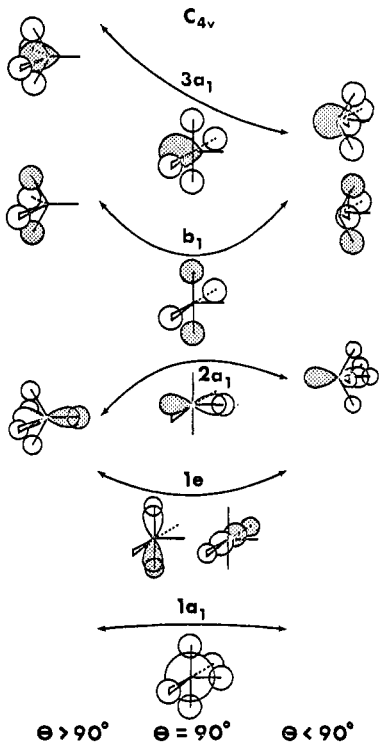

Figure 4. How MO energies change with distortions of the apical-basal angle θ on either side of 90° for the square pyramidal AB_5 structure.

pied MO acts to damp or lower the barrier: $3a_1$ (C_{2v})-b_{1g} (D_{4h}) in AB_4 and $2a_1'$ (D_{3h})-b_1 (C_{4v}) in AB_5. Even these damping MOs have much in common. Both $3a_1$ (AB_4, C_{2v}) and $2a_1'$ (AB_5, D_{3h}) are nonbonding MOs that include central atom AOs. At the transition state, the orbitals b_{1g} (AB_4, D_{4h}) and b_1 (AB_5, C_{4v}) are identical and involve only ligand AOs. This suggests that the ten-electron AB_4 complexes should follow the same rules as AB_5 complexes for predicting relative heights of barriers to pseudorotation. No barriers are known for the AB_4 series. The qualitative MO model cannot predict whether AB_4 barriers should be higher or lower than those for AB_5 but it can explain why the AB_3 complexes, lacking the higher energy barrier-damping MO, should have higher inversion barriers than either AB_4 or AB_5.

Bond Distances and Angles and Substituents

The data for ten-electron AB_5 complexes in Table III show that the axial A-B bonds are slightly longer than the equatorial A-B bonds. The differences are small but consistent. Bond order contributions from individual MOs are proportional to the overlap of AOs on connected atoms multiplied by the product of coefficients of the overlapping AOs. The nodeless MO $1a_1'$ (D_{3h}) is smooth and spherical and ligand AO coefficients are practically equal. The $2a_1'$ orbital is nearly A-B nonbonding because of the small coefficient of the central atom s AO. Greater differences in bond order occur in the orbitals $1a_2''$ ($A-B_{ax}$ bonding only) and 1e' ($A-B_{eq}$ bonding only). The $1e_y'$ orbital (viewed below down the threefold axis) has the

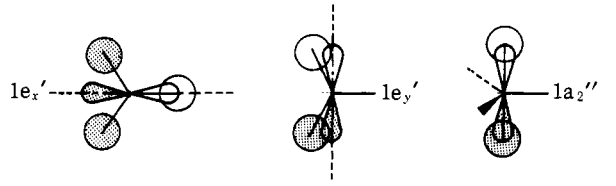

same AO composition as $1a_2''$, but with each ligand tilted 30° away from the central atom p axis in $1e_y'$ the overlap is still 87% (= cos 30°) of the maximum value that is possible in $1a_2''$ (100%). Therefore, one can expect the $A-B_{eq}$ bond order contribution from $1e_y'$ to be about 87% of the $A-B_{ax}$ contribution of $1a_2''$. But $1e_x'$ also contributes to the $A-B_{eq}$ bond order. Considering the same pair of ligands in $1e_y'$, the corresponding ligand AO's in $1e_x'$ are 60° from the central atom p axis, with an overlap that is 50% (= cos 60°) of maximum. The $1e_x'$ orbital contains two ligands AOs of the same phase and, therefore, MO normalization requires that the coefficients of those two AOs be smaller in $1e_x'$ than in $1e_y'$. Still, $1e_x'$ provides a healthy contribution to the $A-B_{eq}$ bond order. The combined overlap fraction for the 1e' pair is 1.37 (= 0.87 + 0.50) compared to 1.00 for $1a_2''$, only slightly larger than the ratio of calculated A-B bond order contributions from 1e' and $1a_2''$ (1.25 for a model AH_5 system). Thus, $A-B_{eq}$ bonds are shorter than $A-B_{ax}$ bonds because the two 1e' orbitals combine to give a larger contribution to $A-B_{eq}$ than the single $1a_2''$ orbital produces for $A-B_{ax}$.

Calculated charge densities are larger at the axial sites than at the equatorial positions. This is a result of MO orthogonality. Suppose we orthogonalize $2a_1'$ (a) against the spherical blob of $1a_1'$. The result requires larger ligand AO coefficients at the axial positions in $2a_1'$ (a) than at equatorial positions. Larger coefficients at the axial sites put larger electron densities there. More electronegative substituents prefer positions where coefficients are larger and which offer greater electron density.

In each 12-electron complex the apical bond is shorter than the basal bonds. The data in Table IV show differences that range from 0.03 to 0.3 Å. The highest occupied MO is $3a_1$ (C_{4v}). Look at the after-mixing picture of $3a_1$ in Figure 2.

Orbital mixing reduces the apical ligand AO coefficient, reducing the $A-B_{ap}$ antibonding nature of $3a_1$. Furthermore, the central atom p AO introduced into $3a_1$ by MO mixing enters in phase with the apical ligand to produce a small bonding component in the $A-B_{ap}$ bond order from $3a_1$. Thus, $3a_1$ is essentially $A-B_{ap}$ nonbonding but still $A-B_{ba}$ antibonding. The b_1 MO makes no contribution to either $A-B_{ap}$ or $A-B_{ba}$ bond orders because this orbital contains no central atom AOs. Compare $2a_1$ with the two 1e orbitals. The AO overlaps are exactly the same in the two different kinds of MOs, but there are two ligand AOs in each 1e orbital but only one ligand AO in $2a_1$. MO normalization requires smaller AO coefficients where there are more AOs. Therefore, the ligand AO coefficient in $2a_1$ will be larger, making the $A-B_{ap}$ bond order contribution from $2a_1$ larger than individual $A-B_{ba}$ bond order terms from the 1e orbitals. In the 12-electron AB_5 complexes $3a_1$ lengthens basal bonds and $2a_1$ shortens the apical bond. For $InCl_5^{2-}$, the ten-electron complex with square pyramidal geometry, the $3a_1$ MO is vacant but $2a_1$ still operates to make the axial bond 0.05 Å shorter than the basal bonds.

The b_1 MO of square pyramidal geometry contains no AO contribution from the apical ligand. The apical coefficient in $3a_1$ (after mixing) is much smaller than those of the basal ligands. Thus, the basal ligand AO coefficients in b_1 and $3a_1$ increase the electron density at the basal positions compared to that at the apical location. Electronegative substituents, preferring the more electron-rich sites, occupy the basal positions in square pyramidal complexes.

The angles between apical and basal bonds are less than 90° in square pyramidal 12-electron complexes. However, in the square pyramidal ten-electron complex $InCl_5^{2-}$ the apical-basal angle is greater than 90°. Figure 4 shows roughly how the MO energies of AB_5 vary as functions of the apical-basal angle θ. The energy of $1a_1$ is nearly constant. The doubly degenerate 1e levels are at an energy minimum at $\theta = 90°$, where there is maximum overlap between ligand AOs and the central atom p orbitals that are perpendicular to the C_4 axis. Distortions from 90° produce a symmetric energy increase which is

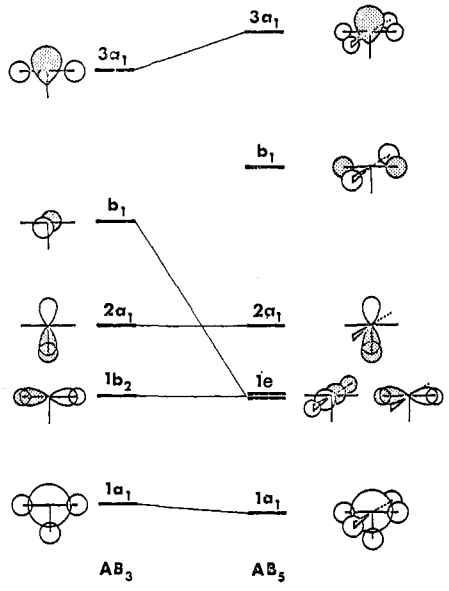

Figure 5. Comparison of MOs of T-shaped AB_3 and square pyramidal AB_5.

proportional to the cosine of the angle of distortion from 90°. For a 10° variation, cos 10° = 0.985 and the energy is quite small. The b_1 orbital also has a symmetric energy minimum at $\theta = 90°$. Variations from 90° push ligand AOs together out of phase and raise the orbital energy. The slope of the energy curve gets ever steeper the greater the angular variation from 90° and, thus, b_1 limits the amount of distortion in 10- and 12-electron complexes. The orbital $2a_1$ has an energy maximum near $\theta = 90°$ where ligand AOs are near if not on the nodal surface of the MO. For $\theta < 90°$ all ligand AOs enter $2a_1$ with the same phase; for $\theta > 90°$ the four basal ligand AOs enter with phase opposite to that of the apical ligand AO. The energy curve of $2a_1$ is not symmetric. When all ligand AOs have the same phase, normalization requires that their coefficients be smaller than when they have different phases. Since larger coefficients produce larger energy changes, $2a_1$ has lower energy on the $\theta > 90°$ side. The angle $\theta = 90°$ is not an extremum for $3a_1$. The energy of $3a_1$ is high for $\theta > 90°$ because the basal ligands are in close out-of-phase overlap with the lone pair lobe pointing out of the base of the pyramid. As θ decreases, these out-of-phase interactions are relaxed and the energy decreases. The slope of this energy decline is steeper where the out-of-phase overlap is greater ($\theta > 90°$).

For ten-electron complexes such as $InCl_5^{2-}$ ($\theta = 108°$), the $2a_1$ MO tends to distort the square pyramid toward $\theta > 90°$. For 12-electron complexes $3a_1$ pushes the basal ligands toward $\theta < 90°$. In both cases b_1 acts to limit these distortions. The qualitative MO model provides a clear prediction of the direction of the distortion from the flat based pyramid.

Comparisons with AB_3, AB_4, and AB_6 Systems

The close similarity between the occupied MOs of T-shaped AB_3 (10e, C_{2v}) and square pyramidal AB_5 (12e, C_{4v}) complexes is shown in Figure 5. Tie lines connect MOs with related AO compositions. The nonbonding b_1 (AB_5) MO holds the additional electron pair of the square pyramidal complexes. Since b_1 (AB_5) contains no central atom AO and b_1 (AB_3) contains no ligand AOs, neither of these MOs affects the A-B bond orders of their respective complex series. The contributions to A-B bond order from $1b_2$ (AB_3) and 1e (AB_5) must be identical because AO compositions and coefficients are identical. The same is roughly true for the two pairs of orbitals $1a_1$ and $2a_1$. Because of the larger number of phase differences in the $3a_1$ orbitals the AO coefficients in these MOs will be larger than those in lower energy orbitals. Therefore, we can

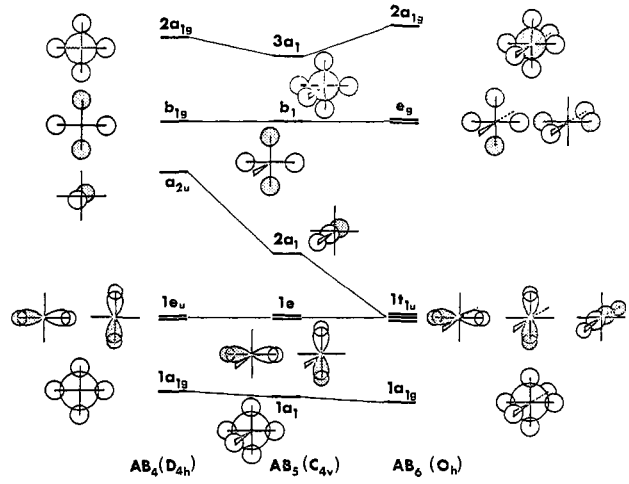

Figure 6. Comparison of MOs of AB_4, AB_5, and AB_6 in square planar, square pyramidal, and octahedral shapes.

Table V. Comparison of A-B Distances in AB_5 and AB_3

	BrF_5[a]	BrF_3[b]	XeF_5^+[c]	XeF_3^+[d]
A-B (basal or T-crossbar)	1.774	1.810	1.845	1.89
A-B (apical or T-upright)	1.689	1.721	1.793	1.83

[a] Reference 33. [b] D. W. Magnuson, *J. Chem. Phys.*, **27**, 223 (1957); R. D. Burbank and I. N. Bensey, *ibid.*, **27**, 982 (1957). [c] Reference 34. [d] D. E. McKee, A. Zalkin, and N. Bartlett, *Inorg. Chem.*, **12**, 1713 (1973); P. Boldrini, R. J. Gillespie, P. R. Ireland, and G. J. Schrobilgen, *ibid.*, **13**, 1690 (1974).

expect the $3a_1$ MOs to be mainly responsible for differences in A-B bond orders between AB_3 and AB_5.

In both $3a_1$ MOs the interactions of the central atom with the basal (AB_5) or T-crossbar (AB_3) ligands are antibonding. In both cases, mixing with a higher a_1 MO makes $3a_1$ nonbonding between the central atom and the apical (AB_5) or T-stem or upright (AB_3) ligands. Because $3a_1$ (AB_3) contains fewer ligand AOs than $3a_1$ (AB_5), MO normalization requires that individual ligand AO coefficients be larger in $3a_1$ (AB_3) than they are in $3a_1$ (AB_5). The differences in magnitudes of ligand AO coefficients and the fact that the A-B interactions are antibonding in both $3a_1$ orbitals results in longer A-B bonds for AB_3 (10e, C_{2v}) than for AB_5 (12e, C_{4v}). Table V compares $A-B_{ba}$ with A-B (T-crossbar) and $A-B_{ap}$ with A-B (T-upright) for the pairs BrF_5, BrF_3 and XeF_5^+, XeF_3^+. The less substituted complex has longer bonds. The same trend is to be expected in the following known pairs for which bond distances of one or both members have not been reported: ClF_5, ClF_3; $SeCl_5^-$, $SeCl_3^-$; $SeBr_5^-$, $SeBr_3^-$. A similar lengthening of A-B bonds with decreasing substitution for AB_6 (14e, O_h), AB_4 (12e, D_{4h}), and AB_2 (10e, linear) has a related MO explanation.[2]

Figure 6 compares the occupied MOs of AB_4 (D_{4h}), AB_5 (C_{4v}), and AB_6 (O_h). As front and then rear ligands are added to the square planar system of AB_4, the energy of nonbonding a_{2u} (D_{4h}) drops to that of bonding $1t_{1u}$ (O_h). The energy of $3a_1$ (C_{4v}) is lower than that of either $2a_{1g}$ (D_{4h}) or $2a_{1g}$ (O_h) because $3a_1$ (C_{4v}) can mix with a higher energy MO of a_1 symmetry to reduce out-of-phase A-B overlaps, a process not possible in the higher symmetry D_{4h} and O_h systems where the $2a_{1g}$ MOs are the highest energy orbitals of their symmetry. The similar nature of the MOs in Figure 6 suggests that these complexes should be formed from similar elements. That this is true, at least for the AB_5 and AB_6 series, can be seen by comparing the pattern of known complexes in Table II with those in related tables in ref 2 and 3. The highest occupied MOs are A-B antibonding but they have in-phase overlaps between

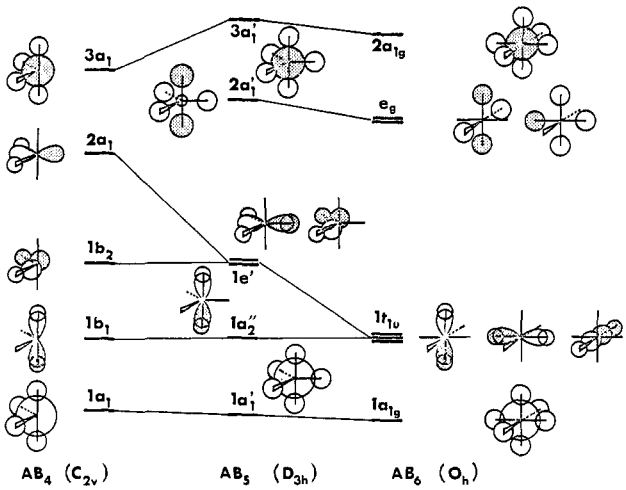

Figure 7. Comparison of MOs of AB_4, AB_5, and AB_6 in folded square, trigonal bipyramidal, and octahedral shapes.

ligand AOs, an arrangement that tends to stabilize complexes with large ligands such as iodides compared to fluorides. Exceptions are those complexes in which the central atom is highly electronegative.[2] Just below the antibonding MO lie nonbonding orbitals which have B-B out-of-phase overlaps and no central atom AO. The number of pairs of B-B in-phase overlaps in the antibonding MOs increases from four pairs in AB_4 to eight pairs in AB_5 to 12 pairs in AB_6. The number of pairs of B-B out-of-phase interactions in the nonbonding MOs is four pairs each in AB_4 and AB_5 and eight pairs in AB_6. Canceling numbers of in-phase and out-of-phase overlaps in AB_4 (12e, D_{4h}) nearly eliminate the entire class, there being only six known examples and nearly every one of those involves only the most electronegative elements.[3] There is greater similarity between the AB_5 and AB_6 systems with in-phase B-B overlaps outnumbering the out-of-phase overlaps. In the ten-electron AB_4 complexes of diagonally folded square (C_{2v}) shape, the MO related to b_{1g} (AB_4, D_{4h}) is empty. These AB_4 (10e, C_{2v}) complexes turn out to have electronic structure and chemical compositions similar to AB_5 (12e, C_{4v}) and AB_6 (14e, O_h).

There are six complexes in the AB_4 (12e, D_{4h}) class, 20 in AB_5 (12e, C_{4v}), and 30 for AB_6 (14e, O_h). Between AB_5 and AB_6 there are 18 related pairs of complexes composed of the same elements such as XeF_5^+ and XeF_6. In other words, for all but two of the known AB_5 (12e, C_{4v}) complexes the related AB_6 (14e, O_h) complex is also known. The similar electronic structure does favor complexes of the same elements.

Figure 7 compares the occupied MOs of AB_4 (C_{2v}), AB_5 (D_{3h}), and AB_6 (O_h). There is much less similarity between MOs of these different structures than we found in Figures 5 and 6. Assuming an angle of 120° between the equatorial ligands of the diagonally folded square (C_{2v}) structure gives $1b_2$ (C_{2v}) and one of the components of 1e' (D_{3h}) identical AO compositions, overlaps, and energies.

The AB_4 (10e, C_{2v}) complexes are often reviewed along with those of AB_5 (10e, D_{3h}) series, the structure of the AB_4 complexes being described as trigonal bipyramidal like AB_5 but with a lone pair of electrons occupying one of the equatorial positions. Despite their geometrical similarity the electronic structures of the two classes of complexes are different enough to make the kinds of complexes contained in the two classes quite different. Consider the differences in the highest occupied MOs at the ten-electron level. In $3a_1$ (AB_4) the axial and equatorial ligand AOs have the same phase which tend to stabilize complexes with large ligands, iodides more than bromides, etc. See ref 3, Table II. On the other hand, $2a_1'$ (AB_5) has axial and equatorial ligand AOs of opposite phase,

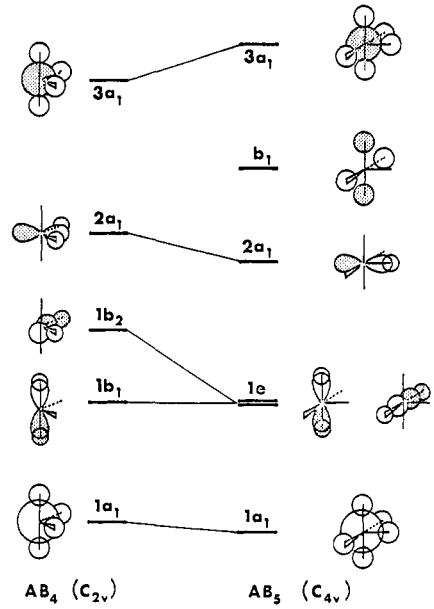

Figure 8. Comparison of MOs of AB_4 (folded square) and AB_5 (square pyramidal).

an arrangement stabilized by small ligands and large central atoms, a conclusion supported by the pattern of known ten-electron AB_5 complexes shown in Table I. Of the 18 AB_5 complexes in Table I, there are nine fluorides, seven chlorides, two bromides, and no iodides. The data here are rather sparse. Only 18 AB_5 complexes with 10 valence electrons are known compared to 32 AB_4 complexes with 10 electrons. Between these two classes of complexes there are only six related pairs such as PF_4^-, PF_5.

Figure 8 compares the electronic structures of AB_4 (10e, C_{2v}) and AB_5 (12e, C_{4v}) complexes. In both classes of complexes the highest occupied MO is A-B antibonding but with B-B in-phase overlaps which favor large ligands. In each class the antibonding $3a_1$ MO is stabilized by mixing with a higher unoccupied orbital to the same symmetry to form an orbital related to the lone pair orbital of the VSEPR model. The similarity of highest occupied MOs suggests that the two classes of complexes should be formed from similar elements. Between 32 known AB_4 (10e, C_{2v}) complexes and 20 known AB_5 (12e, C_{4v}) complexes, there are 19 related pairs, such as SF_4 and SF_5^-.

Summary

Molecular orbitals and their relative energies can be obtained qualitatively following some simple rules. The results can be supported by MO calculations. The MO energies show that 12-electron AB_5 complexes are square pyramidal. The ten-electron series should be trigonal bipyramidal, although some square pyramidal exceptions are known. These exceptions can be understood with a model that also predicts the relative heights of barriers to pseudorotation in the trigonal bipyramidal complexes. Energy level comparisons are made to show the relationship of pseudorotation or inversion barriers in AB_3, AB_4, and AB_5 complexes. Qualitative bond order arguments rationalize the longer axial bonds in trigonal bipyramidal complexes and the shorter apical bonds in square pyramidal structures. Similar reasoning, including MO normalization requirements, explains why Br-F bonds are shorter in BrF_5 than in BrF_3. Qualitative charge density arguments explain why more electronegative ligands prefer axial sites in trigonal bipyramidal complexes and basal positions in square pyramidal structures. Relative stabilities of complexes can be interpreted by considering the properties of the higher occupied MOs. Stabilities of AB_5 complexes can be compared to those of re-

lated series in the AB_4 and AB_6 classes. Qualitative MO theory can act as a great organizing principle for a large body of inorganic chemistry.

Acknowledgment. This research was sponsored by a grant from the National Science Foundation.

References and Notes

(1) B. M. Gimarc, *Acc. Chem. Res.*, **7**, 384 (1974).
(2) B. M. Gimarc, J. F. Liebman, and M. Kohn, accompanying paper in this issue.
(3) B. M. Gimarc and S. A. Khan, accompanying paper in this issue.
(4) E. L. Muetterties and R. A. Schunn, *Q. Rev., Chem. Soc.*, **20**, 245 (1966).
(5) K. W. Hansen and L. S. Bartell, *Inorg. Chem.*, **4**, 1775 (1965).
(6) W. J. Adams and L. S. Bartell, *J. Mol. Struct.*, **8**, 23 (1971).
(7) F. B. Clippard, Jr., and L. S. Bartell, *Inorg. Chem.*, **9**, 805 (1970).
(8) S. M. Ohlberg, *J. Am. Chem. Soc.*, **81**, 811 (1959).
(9) R. F. Bryan, *J. Am. Chem. Soc.*, **86**, 733 (1964).
(10) J. W. Wilmshurst, *J. Mol. Spectrosc.*, **5**, 343 (1960).
(11) G. L. Carlson, *Spectrochim. Acta*, **19**, 1291 (1963).
(12) R. W. Suter, H. C. Knachel, V. P. Petro, J. H. Howatson, and S. G. Shore, *J. Am. Chem. Soc.*, **95**, 1474 (1973).
(13) D. Clark, H. M. Powell, and A. F. Wells, *J. Chem. Soc.*, 642 (1942); H. Gerding and H. Houtgraaf, *Recl. Trav. Chim. Pays-Bas*, **74**, 5 (1955).
(14) W. Gabes and K. Olie, *Acta Crystallogr., Sect. B*, **26**, 443 (1971).
(15) I. R. Beattie, N. Cheetham, T. R. Gilson, K. M. S. Livingston, and D. J. Reynolds, *J. Chem. Soc. A*, 1910 (1971).
(16) C. Hebecker, *Z. Anorg. Allg. Chem.*, **384**, 111 (1971).
(17) K. O. Christe, R. D. Wilson, and I. B. Goldberg, *Inorg. Chem.*, **15**, 1271 (1976).
(18) D. S. Brown, F. W. F. Einstein, and D. G. Tuck, *Inorg. Chem.*, **8**, 14 (1969).
(19) S. R. Leone, B. Swanson, and D. F. Shriver, *Inorg. Chem.*, **9**, 2189 (1970).
(20) J. Gislason, M. H. Lloyd, and D. G. Tuck, *Inorg. Chem.*, **10**, 1907 (1971).
(21) D. M. Adams and R. R. Smardzewski, *J. Chem. Soc. A*, 714 (1971).
(22) D. F. Shriver and I. Wharf, *Inorg. Chem.*, **8**, 2167 (1969).
(23) G. Joy, A. P. Gaughan, Jr., I. Wharf, D. F. Shriver, and J. P. Dougherty, *Inorg. Chem.*, **14**, 1795 (1975).
(24) R. S. Berry, *J. Chem. Phys.*, **32**, 933 (1960).
(25) F. Klauberg and E. L. Muetterties, *Inorg. Chem.*, **7**, 155 (1968).
(26) I. Ugi, D. Marquarding, H. Klusacek, P. Gillespie, and F. Ramirez, *Acc. Chem. Res.*, **4**, 288 (1971).
(27) J. E. Griffiths, R. P. Carter, Jr., and R. R. Holmes, *J. Chem. Phys.*, **41**, 863 (1964).
(28) K. O. Christe, *Inorg. Nucl. Chem. Lett.*, **8**, 457 (1972); K. O. Christe and R. D. Wilson, *Inorg. Chem.*, **12**, 1356 (1973); K. O. Christe and E. C. Curtis, *Ibid.*, **12**, 2245 (1973).
(29) I. R. Beattie and G. J. Van Schalkwyk, *Inorg. Nucl. Chem. Lett.*, **10**, 343 (1974).
(30) G. Gundersen and K. Hedberg, *J. Chem. Phys.*, **51**, 2500 (1969).
(31) R. R. Ryan and D. T. Cromer, *Inorg. Chem.*, **11**, 2322 (1972).
(32) S. H. Mastin, R. R. Ryan, and L. B. Asprey, *Inorg. Chem.*, **9**, 2100 (1970).
(33) A. G. Robiette, R. H. Bradley, and P. N. Brier, *Chem. Commun.*, 1567 (1971).
(34) N. Bartlett, M. Gennis, D. D. Gibler, B. K. Morrell, and A. Zalkin, *Inorg. Chem.*, **12**, 1717 (1973).
(35) M. Webster and S. Keats, *J. Chem. Soc. A*, 298 (1971).
(36) K. O. Christe and E. C. Curtis, *Inorg. Chem.*, **11**, 2209 (1972).
(37) R. R. Ryan and L. B. Asprey, *Acta Crystallogr., Sect. B*, **28**, 979 (1972).
(38) E. J. Jacob, H. B. Thompson, and L. S. Bartell, *J. Mol. Struct.*, **8**, 383 (1971).
(39) J. B. Milne and D. Moffett, *Inorg. Chem.*, **12**, 2240 (1973).
(40) J. R. Morton and K. F. Preston, *Chem. Phys. Lett.*, **18**, 98 (1973); J. Gawlowski and J. A. Herman, *Can. J. Chem.*, **52**, 3631 (1974).
(41) S. P. Mishra and M. C. R. Symons, *J. Chem. Soc., Chem. Commun.*, 279 (1974).
(42) S. P. Mishra and M. C. R. Symons, *J. Chem. Soc., Dalton Trans.*, 139 (1976).
(43) R. Hoffmann, J. M. Howell, and E. L. Meutterties, *J. Am. Chem. Soc.*, **94**, 3047 (1972).
(44) A. R. Rossi and R. Hoffmann, *Inorg. Chem.*, **14**, 365 (1975).
(45) (a) L. S. Bartell, *J. Chem. Educ.*, **45**, 754 (1968); (b) R. G. Pearson, *J. Am. Chem. Soc.*, **91**, 4947 (1969).
(46) J. I. Musher, *J. Am. Chem. Soc.*, **94**, 1370 (1972).
(47) E. M. Shustorovich and Yu. A. Buslaev, *Inorg. Chem.*, **15**, 1142 (1976).
(48) A. Rauk, L. C. Allen, and K. Mislow, *J. Am. Chem. Soc.*, **94**, 3035 (1972).
(49) F. Keil and W. Kutzelnigg, *J. Am. Chem. Soc.*, **97**, 3623 (1975).
(50) J. A. Altmann, K. Yates, and I. G. Csizmadia, *J. Am. Chem. Soc.*, **98**, 1450 (1976).
(51) W. Th. A. M. van der Lugt and P. Ros, *Chem. Phys. Lett.*, **4**, 389 (1969).
(52) P. Cremaschi and M. Simonetta, *Theor. Chim. Acta*, **37**, 341 (1975).
(53) D. L. Wilhite and L. Spialter, *J. Am. Chem. Soc.*, **95**, 2100 (1973).
(54) F. Keil and R. Ahlrichs, *Chem. Phys.*, **8**, 384 (1975).
(55) A. Strich and A. Veillard, *J. Am. Chem. Soc.*, **95**, 5574 (1973).
(56) J. M. Howell, J. R. Van Wazer, and A. R. Rossi, *Inorg. Chem.*, **13**, 1746 (1974).
(57) P. C. Van Der Voorn and R. S. Drago, *J. Am. Chem. Soc.*, **88**, 3255 (1966).
(58) D. P. Santry and G. A. Segal, *J. Chem. Phys.*, **47**, 158 (1967).
(59) R. D. Brown and J. B. Peel, *Aust. J. Chem.*, **21**, 2605 (1968).
(60) R. S. Berry, M. Tamres, C. J. Ballhausen, and H. Johansen, *Acta Chem. Scand.*, **22**, 231 (1968).
(61) J. B. Florey and L. C. Cusachs, *J. Am. Chem. Soc.*, **94**, 3040 (1972).
(62) J. M. Howell, *J. Am. Chem. Soc.*, **97**, 3930 (1975).
(63) M. F. Guest, M. B. Hall, and I. H. Hillier, *J. Chem. Soc., Faraday Trans. 2*, **69**, 1829 (1973).
(64) A. R. Gregory, *Chem. Phys. Lett.*, **28**, 552 (1974).
(65) R. J. Gillespie and R. S. Nyholm, *Q. Rev., Chem. Soc.*, **11**, 339 (1957); R. J. Gillespie, *J. Chem. Educ.*, **47**, 18 (1970); **51**, 367 (1974).
(66) L. S. Bernstein, S. Abramowitz, and I. W. Levin, *J. Chem. Phys.*, **64**, 3228 (1976).
(67) L. C. Hoskins and R. C. Lord, *J. Chem. Phys.*, **46**, 2402 (1967).
(68) R. R. Holmes and R. M. Deiters, *Inorg. Chem.*, **7**, 2229 (1968); R. R. Holmes, R. M. Deiters, and J. A. Golen, *Ibid.*, **8**, 2612 (1969); R. R. Holmes, *Acc. Chem. Res.*, **5**, 296 (1972).
(69) W. G. Klemperer, J. K. Krieger, M. D. McCreary, E. L. Muetterties, D. D. Traficante, and G. M. Whitesides, *J. Am. Chem. Soc.*, **97**, 7023 (1975).
(70) NOTE ADDED IN PROOF. R. Hoffmann and E. Shustorovich (private communication) point out that the ratio of sizes of axial and equatorial ligand orbital coefficients in a is $^3/_2$ from first-order perturbation theory. This ratio just compensates for the $^2/_3$ ratio of numbers of $A-B_{ax}$ out of phase to $A-B_{eq}$ in phase interactions in a.